Journal of Physiology (1988), **402**, *pp.* 751–771
With 8 text-figures
Printed in Great Britain

EFFECTS OF ELECTRIC FIELDS ON TRANSMEMBRANE POTENTIAL AND EXCITABILITY OF TURTLE CEREBELLAR PURKINJE CELLS *IN VITRO*

BY C. Y. CHAN*‡, J. HOUNSGAARD† AND C. NICHOLSON*

*From the *Department of Physiology and Biophysics, New York University Medical Center, 550 First Avenue, New York, NY 10016 and †Institute of Neurophysiology, University of Copenhagen, Blegdamsvej 3C, DK-2200 Copenhagen N., Denmark*

(*Received 8 September 1987*)

SUMMARY

1. Transmembrane potential (TMP) responses of Purkinje cells (PCs) in isolated turtle cerebellum to externally applied quasi-steady-state electric fields aligned with the dendritic axis were continuously measured using simultaneous intracellular and extracellular recording. TMP was obtained by subtraction of extracellular voltage fields from intracellular potential recorded at the same depth in the cerebellum.

2. The applied field changed the TMP with the polarity and amplitude dependent on the location on the PC membrane. This response at a given location increased linearly with external field up to a threshold level, beyond which active responses appeared.

3. The basic effect on TMP consisted of depolarization in the half of the dendrite towards which the fields were directed, and hyperpolarization in the other half. A pooled TMP depth-profile shows a steady increase in polarization from the middle of the molecular layer towards each end. This profile correlates with that predicted from previously proposed cable models, giving them empirical support for the first time.

4. Active responses were triggered by the field-induced depolarization. Tetrodotoxin (TTX)-sensitive action potentials arose with the primary depolarization in the somatic region. Notched, Ca^{2+}-dependent action potentials arose with primary depolarization in the distal and mid-dendritic regions.

5. A TTX-sensitive voltage plateau was triggered by TMP-depolarization in the proximal region. It in turn activated Na^+-spike trains. The frequency of spiking was proportional to the external field. At around 160 spikes/s, the Na^+ spikes inactivated, and the TMP level rose to a more depolarized plateau. This latter plateau was also TTX-sensitive.

6. During depolarization of the distal dendritic region, sometimes a Ca^{2+}-dependent plateau was observed. It appears to be associated with a small conductance increase.

7. Field-induced hyperpolarization suppressed local spiking and voltage plateaux,

‡ Present address, to which reprint requests should be sent: Department of Physiology, CUNY Medical School, Convent Avenue and 138th Street, New York, NY 10031, U.S.A.

but remote Ca^{2+} spikes with reduced amplitude appeared in recordings from the proximal region. Similarly, in the distal region, low-amplitude, remote Na^+ spikes and a Na^+ plateau were observed superimposed on the hyperpolarizing baseline. The Na^+ plateau apparently did not contribute to shunting of membrane currents in the distal dendrite.

8. The phase characteristics of the action potentials correlate with the modulation pattern noted in our extracellular study (Chan & Nicholson, 1986). Thus, the extracellular units ('giant spikes') were probably Na^+ spikes activated in the soma and spread distally. Occasionally Ca^{2+} spikes, with a higher threshold, might also be activated to give a dual-phase response. The voltage plateaux were probably the mechanism underlying some of the burst patterns observed.

9. The characteristics of these active responses elicited by external field application were very similar to those elicited by current steps injected via a microelectrode into turtle PCs (Hounsgaard & Midtgaard, 1988) and guinea-pig PCs (Llinás & Sugimori, 1980*a*, *b*), confirming the effectiveness of external field as a novel membrane electrophysiological tool. When both intracellular current injection and external field were applied simultaneously, their effects were shown to be additive.

INTRODUCTION

The technique of applying electric fields across neural tissues in order to stimulate populations of central neurones, when used in conjunction with intracellular recording, provides a new approach to the study of membrane and circuit properties in the CNS. In addition, the method has applications to problems of applied neural control (neuronal prostheses).

Electric fields have been used occasionally to activate deep-lying cell masses from the brain surface (Gauthier, Mollica & Moruzzi, 1956; Purpura & McMurtry, 1965; Purpura & Malliani, 1966). But these studies lacked rigorous definition of the field or its mode of action on neurones. These experimental efforts were supplemented by some theoretical studies of the issues involved (Sten-Knudsen, 1960; Ranck, 1975).

Recently we began a re-investigation of this topic. Using the isolated turtle cerebellum, we were able to rigorously define the characteristics of our applied electric field and demonstrate that the firing patterns of identified Purkinje cells and stellate interneurones were modulated by applied fields in a manner that depended on their dendritic orientation with respect to the field (Chan & Nicholson, 1986). Further support for this work was provided by a detailed theoretical study (Tranchina & Nicholson, 1986).

Here we study the mechanism of modulation of Purkinje cell activities by electric fields through direct measurement of transmembrane potential. Our first goal was to examine the polarizing effect of electric fields on the neuronal membrane, characterizing the basic responses of the cable structures and the thresholds for the active responses observed in our previous extracellular study (Chan & Nicholson, 1986). Our second goal was to study the field-elicited active responses in detail. These studies complement those of Hounsgaard & Midtgaard (1988) using conventional cellular electrophysiological techniques in the same preparation.

The advantages of the field application technique as a cellular electrophysiological tool, as compared to local polarization via an intracellular microelectrode, are much more intense membrane polarization, and the possibility of depolarizing or hyperpolarizing regions remote from the intracellular recording site, which would make it a valuable technique in localizing an active membrane event such as synaptic input. In addition, differential polarization assists localizing non-homogeneously distributed membrane properties.

Parts of the data reported below have appeared in a previous abstract (Chan, Hounsgaard & Nicholson, 1985).

METHODS

Much of the procedure for tissue preparation, field application and mapping was similar to that described previously (Chan & Nicholson, 1986). Turtles, species *Psuedemys scripta elegans* or *Chrysemys picta*, with shell length of 12–15 cm and of either sex were decapitated under anaesthesia by an I.P. injection of sodium pentobarbitone (50 mg/kg). The cerebellum was removed into a physiological saline appropriate for the turtle (in mM): NaCl, 120; KCl, 5; $NaHCO_3$, 35; $CaCl_2$, 3; $MgCl_2$, 2; glucose, 20; bubbled with 5% CO_2, 95% O_2. The pia was dissected away from the dorsal surface. The isolated cerebellum was then supported dorsal side up on a nylon mesh stretched over a hole in the partition dividing two compartments of a Perspex chamber. Standard saline or saline solutions containing pharmacological agents were gravity fed through the compartments and removed by continuous suction. Two Ag–AgCl plate electrodes of 2 cm^2 were positioned in the two compartments such that they faced the ventral and dorsal surfaces of the cerebellum. The top plate contained a cut-out to allow access of microelectrodes to the cerebellum during field application between the plates. For field application, quasi-DC sinusoidal currents of ± 2 to 10 mA amplitude and 0·1 Hz were passed between the plates from an isolated current source. The hole over which the cerebellum was suspended was substantially larger than the cerebellum. This was designed to allow most of the current to flow around the cerebellum thus reducing the influence of the edge of the hole on the field in the tissue. Theoretically speaking, the cerebellum can be represented as being embedded in an effectively infinite medium (see Chan & Nicholson, 1986).

The preparation was also set up for synaptic activation of the PCs by two pairs of bipolar platinum surface electrodes. One pair was placed on the dorsal surface to locally activate parallel fibres; the other was placed on the ipsilateral cerebellar peduncle. These electrodes were also energized by isolated constant-current sources (W.P.I. No. 305). Alternatively, the ipsilateral peduncle was stimulated by suction electrodes when special salines or drugs were not used.

Extracellular potentials were recorded using glass micropipettes with tip size of about 1 μm, and filled with 0·25 M-NaCl and 0·25 M-sodium citrate. The shank of the micropipette was bent at a slight angle so that the final section was aligned parallel to an intracellular glass micropipette. The two micropipettes were held in a double micromanipulator (Narishige MD5) and spaced about 50–100 μm apart. This allowed movement of the micropipettes individually or in consort. Potentials were measured against an Ag–AgCl–1 M-KCl–Agar indifferent electrode and the signals amplified by a DC-coupled amplifier.

Intracellular recording was performed using micropipettes with sub-micrometer tip filled with 4 M-$K(CH_3COO)$ (40–70 MΩ). Pulses of low-amplitude alternating current at 1–10 kHz frequency ('tone-bursts') were passed through the micropipette tip to facilitate penetration and sealing of the cell membrane around the tip. Typically, after initial adjustment (see below), the two micropipettes were advanced together. Purkinje cells (PCs) were recognized both on the basis of the depth of recording and by their electrophysiological characteristics, such as a large synaptic potential with broad spikes in response to peduncular stimulation, and a reduction in the spiking response to repeated local parallel fibre activation. The criteria for accepting a penetration were a stable resting potential of at least 50 mV, a membrane time constant of at least 6 ms and the ability of the neurone to generate repetitive action potentials in response to a 50 ms outward current pulse. A conventional active bridge amplifier was used and the bridge balance was continuously adjusted to exclude the voltage artifact caused by current flowing through the electrode tip resistance.

Transmembrane potential was measured by continuously subtracting the output of the extracellular DC amplifier from the output of the intracellular amplifier, using a difference amplifier with a gain balance (Fig. 1*A*). A calibration pulse injected in the ground circuit was used for adjusting the gain balance. The capacitive compensations in the two amplifiers were also set to match during this initial adjustment.

To ensure that both micropipette tips recorded the same field gradient, the following procedure was undertaken for every track. Both tips were aligned so that they were parallel to each other and entered the tissue simultaneously. A sinusoidal field was applied across the tissue, and the depth of one tip was adjusted until no sinusoidal waveform appeared in the output of the difference amplifier. Usually, this only took a small adjustment and few readjustments were necessary throughout the track. Nevertheless, periodic checks were performed.

After penetration of the cell, local polarization could be applied also through the intracellular micropipette using currents of either polarity via the balanced bridge circuit.

Field mapping was performed for every cerebellum used as in the previous study (Chan & Nicholson, 1986). A constant-current step was periodically passed between the plate electrodes, and the extracellular field gradient generated in the cerebellar tissue was measured by advancing one of the two electrodes through 50 μm steps. The gradient was typically constant, and the electric intensity (voltage gradient per unit current) was obtained, and used during subsequent analysis of that cerebellum as a conversion factor to calculate field strength from current strength, since our previous study showed that these two parameters were linearly related through the electric intensity.

In some experiments, a modified physiological saline was used as the superfusate. It contained low Ca^{2+} (0·2 mM), elevated Mg^{2+} (6 mM) with 1 mM-Mn^{2+} (low-Ca^{2+}–Mn^{2+} saline). The other ionic species were unchanged. In another set of experiments, tetrodotoxin (TTX, 1 mM stock solution in H_2O) was added directly to the normal or low-Ca^{2+}–Mn^{2+} saline in the recording chamber to obtain an estimated final concentration of 1–3 μM.

RESULTS

Subthreshold transmembrane polarization associated with extracellular electric fields

Our first aim was to verify the hypothesized membrane polarization by external electric fields. Initial measurements were made with fields of lower amplitudes than were required to elicit firing. In subsequent experiments, larger fields were applied to show that the passive response increased with field intensity and elicited active responses.

TMP was measured by penetration of physiologically identified PCs at various depths from the pia surface. After the resting potential had stabilized, a 0·1 Hz sinusoidal field was applied along the pia–ventricle axis and monitored by the extracellular microelectrode. The TMP response to the applied fields measured at various depths in the molecular layer fell into a consistent pattern, as illustrated in Fig. 1*B*. In the shallower region from the pial surface to 180 μm below (*B* 1), a sinusoidal TMP fluctuation was observed phase-locked to the external field: the TMP was depolarized when the field was oriented in the ventricle-to-pia direction and hyperpolarized when the field direction was reversed. There was no TMP polarization at the time of field reversal.

In the deeper region (from 300 to 400 μm), the TMP perturbations associated with the field were also sinusoidal and phase-locked to the field but 180 deg out of phase with that in the distal region (*B* 3). A ventricle-to-pia oriented field was associated with hyperpolarization of the TMP. Here again, the TMP was not polarized at the moment of reversal of field direction, indicating no delayed effect of the field on the TMP observable at the 100 ms time scale.

In the mid-molecular layer (180–300 μm), which corresponds to the mid-dendritic level of the PC, TMP perturbation was much lower in amplitude and appeared to be phase-locked to the field; however, the phase relation may resemble either of the two other regions, probably reflecting the actual geometry of the dendritic tree under study.

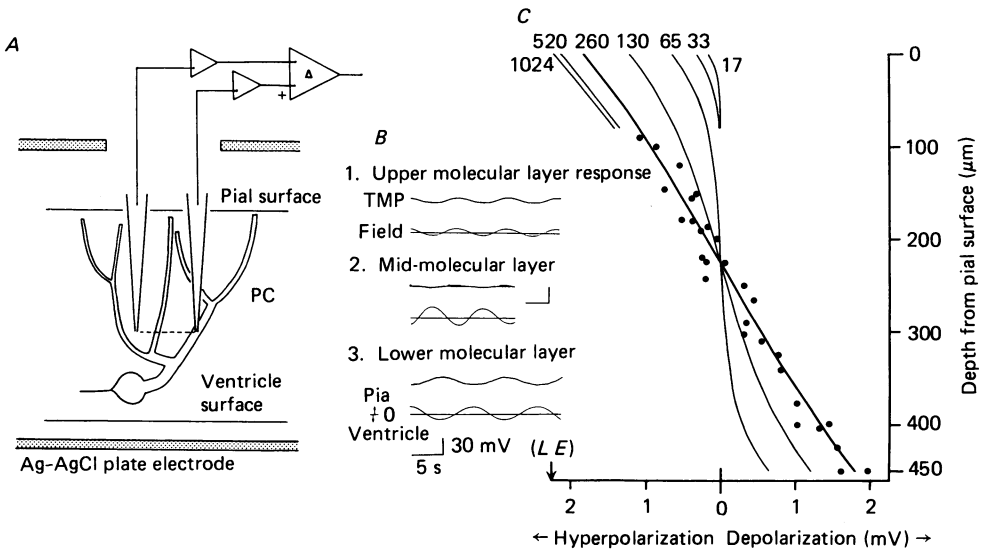

Fig. 1. Measurement of subthreshold TMP perturbation by extracellular field. *A*, schematic drawing (not to scale) showing method of TMP measurement by subtraction of extracellular from intracellular potential. Dashed line indicates same depth of microelectrode tips. The length of PC dendritic trees is typically 450 μm. The thickness of cerebellum is 1 mm. *B*, subthreshold responses (top traces) to extracellular fields (bottom traces) measured at different depths corresponding to upper, mid-dendritic tree, and lower dendrite or soma. Note sinusoidal waveform, amplitudes and different phase relationship to field. *C*, depth profile of subthreshold TMP responses to field by a number of PCs. Each recording (●) was normalized to correspond to a 10 mV/mm field for comparison (see justification in text). Continuous lines are theoretical depth profiles constructed from the following equation (Chan & Nicholson, 1986), using values of external field of 10 mV/mm, dendritic length of 450 μm, and space constants of multiples of 17 (up to 1024) μm:

$$V = \lambda E \sinh(x/\lambda - L/\lambda)/\cosh(L/\lambda),$$

where V is the TMP perturbation by field, E the extracellular field strength, x is the distance co-ordinate, λ is the space constant and $L = 0{\cdot}5 \times$ dendritic length. Time and voltage calibration bars in *B* 2 represent same values as in *B* 3. Time and voltage scales in *B* 2 apply to *B* 1.

The depth profile of the membrane polarization associated with field application was further analysed using measurements from twenty-nine PCs impaled at various depths used for measurement above spike threshold (see below). For each penetration of a PC dendrite, we measured the difference between two TMP values which were below the voltage at which observable active responses (e.g. spiking) were elicited by the field. Then the difference between the two corresponding values of external field (i.e. the strength of the field at the same two time points for the TMP measurements)

as well as the depth of penetration were noted. Such measurements restrict the analysis to the passive TMP response component. The TMP change associated with each of these arbitrary field differences was normalized to a value corresponding to a field difference of 10 mV/mm, for the purpose of comparison with other measurements. Such normalization was justified by the linear relationship between TMP perturbation and the magnitude of the extracellular field in the absence of active membrane responses, as reflected by the sinusoidal TMP response to 'subthreshold' sinusoidal fields (Fig. 1*B*).

The normalized TMP changes were plotted against the depths of penetration in Fig. 1*C* for responses to a pia-to-ventricle field. Consistent with the absence of rectification in the TMP responses (Fig. 1*B*), the depth profile of normalized responses to a ventricle-to-pia field was a mirror image about the resting value (i.e. when no field was applied), and was not shown. Using a cable model discussed previously (see Fig. 12 in Chan & Nicholson, 1986), we calculated the expected depth profiles of TMP passive polarization by applied fields based on a dendritic length of 450 μm and various values of space constant. We superimposed these theoretical curves on the experimental profile in Fig. 1*C*. There appears to be an agreement between the theoretical curve based on a space constant of 260 μm and the experimental depth profile, supporting the cable model proposed earlier.

Data from individual neurones show that when the TMP changes induced by the fields exceeded the passive range they showed deviations from the sinusoidal response. Spikes and voltage platforms appeared and the rate of change in TMP generally decreased (e.g. Figs 2*A* 1 and *B* 1, and 3*A* 1, *B* 1, and *C* 1). When the field-elicited active responses were chemically blocked (see below), large sinusoidal TMP perturbations exceeding the normally subthreshold range were unmasked (e.g. Fig. 3*B* 2), suggesting passive membrane polarization as the basic mechanism underlying the active voltage-dependent responses.

Passive TMP polarizations were unaffected by blockade of synaptic transmission using low-Ca^{2+}–Mn^{2+} saline. Figure 4*B* 2 and *C* 2 illustrates a lack of change in the pattern of baseline TMP at the maximum and minimum of the response to a sinusoidal field in low-Ca^{2+}–Mn^{2+} saline ($n = 4$). The data suggest that the sinusoidal responses were independent of synaptic input, and further support PC membrane polarization by the external field as the basic mechanism for field modulation of PC activities.

The waveform of the extracellularly recorded voltage response to the applied currents (i.e. the applied, or more accurately, induced field in the tissue) was not observed to be significantly changed during transmembrane potential events such as spiking, voltage plateaux and pharmacological blockade of them, as illustrated in Figs 2 and 3. This finding confirms that the induced field in the extracellular space is the direct cause but not the effect of passive and active TMP responses.

Effects of extracellular electric fields on active membrane properties

Simple spikes. When the amplitude of the extracellular electric field was gradually increased past the range that elicited passive TMP perturbation, bursts of action potentials were recorded intracellularly from all levels in the molecular layer. Their waveform, duration and rise time as well as phase relationship with the sinusoidal

TMP perturbation varied, depending on the depth of the intracellular recording site, even though the spike bursts had similar frequencies at the same field strength and a similar phase relationship with the external field, i.e. around the maximum of a pia-to-ventricle oriented field.

An example of the TMP response recorded near the PC soma (405 μm) is shown in Fig. 2*A* 1. Large-amplitude, fast-rising action potentials with duration under 2 ms (detail shown in Fig. 2*C* 1) riding on the peak of membrane depolarization appeared when the field was directed towards the ventricle. Responding to the same field

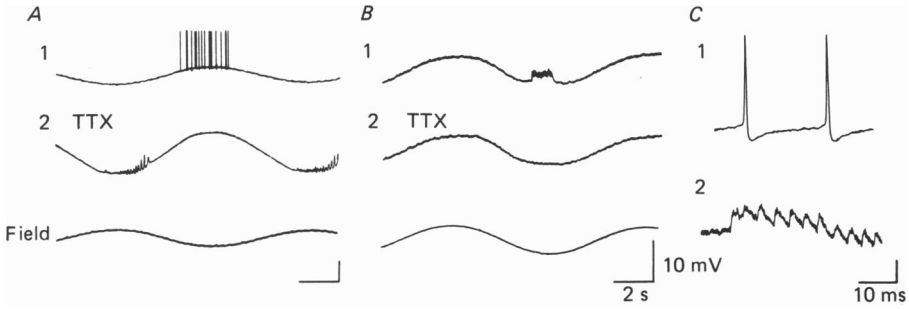

Fig. 2. Nature of simple somatic action potentials induced by external field. *A*, TMP recorded at 425 μm below the pial surface. *A* 1 shows simple spikes occurring at peaks of induced depolarization. Field strength, 54 mV/mm. *A* 2 shows the blocking of these spikes by 1–3 μM-TTX despite a larger (2·4 ×) field strength. Note absence of blocking of baseline polarization. Persisting spikes at higher field strength were dendritic spikes. *B*, TMP recorded at 150 μm below pia in low-Ca^{2+}–Mn^{2+} saline. *B* 1 shows low-amplitude spikes, which disappeared when 1–3 μM-TTX was added to the same saline (*B* 2). The waveforms of spikes in *A* 1 and *B* 1 are shown in *C* 1 and *C* 2, respectively. The waveform in *C* 2 was unchanged when low-Ca^{2+}–Mn^{2+} saline was replaced by normal saline (not shown). Voltage calibration bars in *A* and *C* represent same value as in *B*. Time calibration bar in *A* represents same value as in *B*.

orientation, simple spikes were also recorded in dendritic sites near the pial surface (e.g. Fig. 2*B* 1, recorded at 150 μm). These spikes were however of lower amplitude, slower rise time (Fig. 2*C* 2), and associated with peak membrane hyperpolarization. These data are consistent with a deep-lying (somatic and possibly also primary dendritic) site of spike discharge, which spreads electrotonically to the distal dendrites.

These simple spikes recorded at all depths persisted in low-Ca^{2+}–Mn^{2+} saline ($n = 4$, e.g. Fig. 2*B* 1), but were blocked by about 1–3 μM-tetrodotoxin (TTX) ($n = 5$, e.g. Fig. 2*A* 2, and *B* 2), showing their dependence on Na^+ but not Ca^{2+}.

TTX-sensitive voltage plateau. The rate of Na^+ spikes increased with the strength of the applied pia-to-ventricle fields as described for extracellularly recorded units (Chan & Nicholson, 1986). At higher spiking rates than those shown in Fig. 2*A*, the baseline TMP throughout the duration of the train of Na^+ spikes appeared either flattened or as an elevated platform. These voltage 'plateaux', observed in twenty-eight PCs, are illustrated in Fig. 3*A* 1.

The voltage plateaux observed near the soma consistently appeared flatter than those observed more distally, as shown by the baseline potentials during spiking in

Figs 3*A* 1 and *C* 1 and 4*A* 1. This observation, combined with the fact that these plateaux were associated with the phase of the sinusoidal fields that depolarized the soma, and that inward transmembrane current pulses injected near the soma were sufficient to block the plateaux (Fig. 3*A* 2, described below), indicated that the location of these plateaux was at or near the soma, and electrotonically spread to more distal portions of the dendrite. The current underlying the voltage plateau at the soma was apparently very strong, since voltage plateau waveforms, similar to

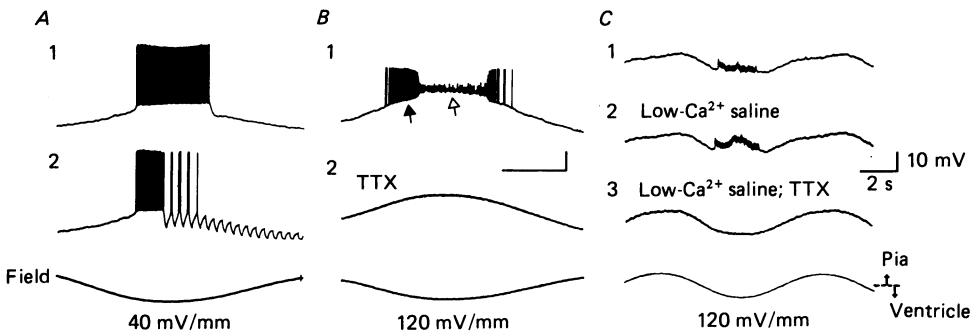

Fig. 3. Nature of somatic voltage plateaux induced by external field. *A*, simple spikes and voltage plateau at the peak of depolarizing TMP response to a pia-to-ventricle field. Recording site was 470 μm below pia. Note continued increase of extracellular field during plateau (bottom trace). *A* 2 shows that inward transmembrane current pulses (2 nA, 100 ms) injected by the intracellular microelectrode hyperpolarized the TMP and interrupted the voltage plateau. Re-establishment of the plateau with spikes followed the cessation of each pulse. *B* 1 shows both the voltage plateau (filled arrow) and a plateau associated with Na^+ spike inactivation (open arrow). The spikes and voltage plateaux disappeared in saline with 1–3 μM-TTX (*B* 2). Recording site was 425 μm below pia. *C*, at a distal dendritic site (150 μm below pia), a plateau waveform occurred during baseline hyperpolarization (*C* 1), which persisted in low-Ca^{2+}–Mn^{2+} saline with a slightly higher amplitude (*C* 2), but was blocked by addition of 1–3 μM-TTX. Calibration bars for voltage and time in *B* represent same values as in *C*. Time and voltage scales in *B* apply to *A*.

that shown in Fig. 3*C* 1, were observed from dendrites at sites as distal as 30 μm below the pial surface ($n = 1$).

This voltage plateau was observed in recordings near the soma (Fig. 3*A* 1 and *B* 1, filled arrow only) or at superficial levels (Fig. 3*C* 1) when the fields were oriented from pia to ventricle. The plateau appeared to be voltage dependent in that the TMP level at its onset was fixed for a given PC, but it was independent of further increases in the amplitude of the sinusoidal applied field so long as the minimum field strength required for its onset was reached. We tested the voltage dependence by passing hyperpolarizing pulses (2 nA, 100 ms) directly into the neurone through the intracellular recording microelectrode placed near the soma level (two experiments). During each of the pulses, the TMP showed polarization and the action potentials were blocked (Fig. 3*A* 2). At the cessation of each pulse, the potential returned towards the depolarized level. The recovery of the membrane potential showed an additional faster-rising section that did not resemble an exponential curve as would be expected of simple discharging, suggesting reinitiation of a voltage plateau,

followed by simple spikes. This modulation of TMP responses to the field by injected currents supports the voltage dependence of these voltage plateaux.

When TTX was added to the bath, both the voltage plateau and the simple spikes were blocked, exposing the usual sinusoidal TMP waveform ($n = 5$, e.g. Fig. 3*B* 2 and *C* 3), suggesting that the voltage plateau is Na^+ dependent. It remains unclear, however, whether TTX directly blocked the voltage plateau or acted indirectly by blocking the action potentials. It appears unlikely that the plateau was due to a field-elicited closing of K^+ or Cl^- channels, as we observed decreases in membrane input resistance during the plateau (measured by small injected current pulses, not shown). These plateaux persisted in low-Ca^{2+}–Mn^{2+} saline and in fact typically responded by an enhancement of the amplitude ($n = 4$, Fig. 3*C* 2). This is consistent with the enhancement of TTX-sensitive voltage plateaux reported in mammalian (Llinás & Sugimori, 1980*a*) and turtle (Hounsgaard & Midtgaard, 1988) PCs.

Voltage plateau observed during somatic spike inactivation. When the amplitude of a pia-to-ventricle field that was sufficiently high to elicit a TTX-sensitive voltage plateau was further increased, the amplitude of the Na^+ spikes diminished abruptly and in some cases the spikes disappeared intermittently or altogether. The frequency and duration of these apparently inactivated Na^+ spikes were both slightly increased. While the spike amplitude was decreasing abruptly, the baseline potential also became more depolarized and formed another voltage plateau ($n = 15$; Fig. 3*B* 1, open arrow; Fig. 4*A* 2). Except for a slight gradual decline from the depolarized level, this plateau held up at a rather constant level while the external field continued to increase and then decrease in magnitude. The spikes then rapidly recovered and the baseline potential also returned to the less depolarized TTX-sensitive plateau level (filled arrow, Fig. 3*B* 1). However, the spiking rate was usually lower after recovery from inactivation and spiking terminated at a more depolarized TMP than at the onset of spiking (Figs 3*B* 1, 4*A* 2 and 5*A* and *B*).

Tetrodotoxin, which blocked the simple spikes and the presumed Na^+ plateau, also blocked this voltage plateau that was always observed during field-induced somatic spike inactivation ($n = 5$; Fig. 3*B* 2), suggesting either that this plateau is due to a Na^+-dependent plateau current that shunts out other ionic currents causing inactivation of spiking, or that it is a direct effect of spike inactivation. The slight decline in depolarization throughout this plateau and the apparent rise in the spiking threshold after recovery from the plateau may be due to a non-inactivating K^+ current. Similar inactivation-associated plateaux could be elicited by a relatively large current pulse injection near the soma (C.Y. Chan, unpublished data). Such plateaux did not continue after the cessation of the injected pulse, as was the case for Na^+ plateaux in the guinea-pig PC (Llinás & Sugimori, 1980*a*, *b*).

Ca^{2+}-dependent dendritic spikes and plateau. Fields at about 2–4 times the strength required to elicit simple spikes and with the opposite orientation, i.e. from ventricle to pia, elicited action potentials that usually showed a complex configuration (with spikelets) and a longer duration (from 5 to over 10 ms; Fig. 4*B*). The amplitudes of these spikes were large at the dendritic level (more than 40 mV). These spikes had fast rise time, and they occurred at or more often lagging behind the peak of TMP depolarization, possibly due to a transient outward current. In contrast, complex spikes recorded close to the soma were smaller in amplitude and had slower rise time.

They were elicited by the same phase of the field, but due to the location on the dendritic axis, the associated baseline TMP was hyperpolarized (Fig. 4*A* 2). Those complex spikes recorded at the lower half of the dendrite were smaller than the more distally recorded ones but otherwise resembled the latter in waveform (Fig. 4*C* 1). These data suggest that the complex spikes occur in the upper part of the dendrite and spread electrotonically to the soma.

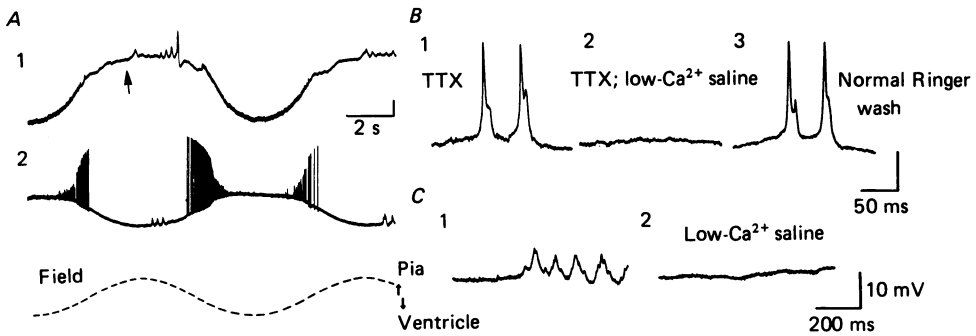

Fig. 4. Dendritic spikes and voltage plateau. *A* 1, a voltage plateau (arrow) and action potentials occurred in the depolarized phase of TMP response (to a ventricle-to-pia field) recorded in a distal dendritic site. *A* 2 shows that in a lower dendritic site, smaller spikes but no plateau occurred in response to the same field. Note that, in contrast, an attenuated somatic plateau is evident in *A* 1. *B*, detail of dendritic spikes recorded in the distal dendritic region of another PC. These traces are taken from the peak depolarizing TMP response. Note notched shape. These spikes persisted in TTX (*B* 1) but were blocked by low-Ca^{2+}–Mn^{2+} saline, which spared the baseline depolarization (*B* 2). The blockade was reversible (*B* 3). *C* 1 shows the waveform of dendritic spikes recorded near the soma. The traces in *C* were taken from the peak hyperpolarizing TMP baseline. The spikes but not the baseline hyperpolarization were blocked by low-Ca^{2+}–Mn^{2+} saline (*C* 2). Calibration bars for voltage in *A* and *B* represent same value as in *C*.

It should be pointed out that we often observed a transient hyperpolarization after a complex spike or a spike burst, consistent with dendritic spikes recorded in guinea-pig and turtle (Llinás & Sugimori, 1980*b*; Hounsgaard & Mitgaard, 1988). These transients have been attributed to a Ca^{2+}-activated K^+ current.

When a strong ventricle-to-pia field was used, a voltage plateau could be observed from a dendritic recording ($n = 6$; e.g. Fig. 4*A* 1, arrow). However, we have not been able to discern from proximal recording a similar, or smaller voltage plateau associated with the same field orientation (Fig. 4*A* 2).

Complex spikes recorded at various levels were sensitive to low-Ca^{2+}–Mn^{2+} saline (Fig. 4*B* 2 and 5) but they persisted in TTX in four cells tested (Fig. 4*B* 1). The plateaux were also reversibly blocked by low-Ca^{2+}–Mn^{2+} saline ($n = 3$; not shown).

Interaction between applied field and injected currents

In order to support further our finding that applied fields exert their major effect through membrane polarization, we observed the combined effect of applied fields and DC current injection through the intracellular recording microelectrode to

determine whether the two effects are integrated at the dendritic membrane. Since the spatial characteristics of membrane polarization by the two methods are very different, we determined the interaction of their effects at various locations in the dendritic tree.

Proximal location. Near the soma, injected inward transmembrane currents during field application generally hyperpolarized the TMP at all phases and had a suppressing effect on the rate of Na^+ spikes and TTX-sensitive voltage plateaux ($n = 8$). This is illustrated in Fig. 5. A sinusoidal field elicited a sinusoidal TMP response and Na^+ spikes at the depolarized phase (Fig. 5*A* 1). At a higher field strength, the Na^+ spikes occurred at a higher rate and showed inactivation during maximal depolarization. Two voltage plateaux associated with spiking and inactivation also occurred, resembling the TTX-sensitive voltage plateaux described above (Fig. 5*A* 2).

When a DC inward transmembrane current was injected through the recording microelectrode during the application of a large field (Fig. 5*B* 2), the TMP was generally hyperpolarized but, other than removal of the plateau, the range of the baseline TMP excursion was little changed, suggesting an additive interaction between the field-elicited and injected current-elicited passive membrane polarization. The active response at the depolarized phase, however, was diminished to resemble those at lower field strength (cf. Fig. 5*A* 1), consistent with a reduced level of membrane depolarization.

The interaction between the effect of applied field and injected outward transmembrane current is illustrated in Fig. 5*C* 1–3 (seven experiments). At constant field amplitude, an increase in outward current strength intensified the passive and active membrane responses (Fig. 5*C* 2). The voltage plateau associated with somatic spike inactivation was lengthened. Furthermore, low-amplitude, slower-rising spikes, resembling dendritic spikes, appeared at the phase of the field that hyperpolarized the proximal dendrite. The amplitude of these spikes recorded at this depth and their phase relationship to the field as well as their higher threshold relative to the simple spikes enabled us to identify them as dendritic spikes (see above). Furthermore, the train of dendritic spikes showed a progressive increase in amplitude as the baseline membrane potential became less hyperpolarized (Fig. 5*C* 2 and *D* 1), consistent with electrotonic spread from a distant active site. The train showed a marked delayed onset, as had been observed before in mammalian and turtle PC dendrites (Llinás & Sugimori, 1980*b*; Hounsgaard & Midtgaard, 1988).

Figure 5*C* 3 shows that an even stronger outward transmembrane DC current, injected through a microelectrode, added a depolarizing bias on the hyperpolarizing phase of the TMP. Its effect on the depolarizing phase was a further lengthening of the inactivation-associated plateau without further depolarization. Somatic spikes persisted at a higher rate near the end of the plateau, but the initial burst before inactivation was obscured by a new spiking pattern in the hyperpolarizing phase: here, the train of dendritic spikes showed an earlier onset and a higher rate. More strikingly, each dendritic spike was associated with one or more fast, somatic-spike-like simple spikes that rode on top of them and reached the same peak potential as the somatic spikes (Fig. 5*D* 2, see also *D* 1). At the less hyperpolarized phase, these

simple spikes occurred ahead of the dendritic spikes, and increased their firing rate until they became inactivated at the peak of each dendritic spike (Fig. 5*D* 3). It is clear from Fig. 5*D* 3 that the dendritic spikes never reached full amplitude, even when the proximal dendritic membrane was not intensely hyperpolarized. These results demonstrated a dynamic interaction between the somatic and dendritic spiking mechanism, and showed the ability of electrotonically conveyed dendritic spikes to cause somatic spiking.

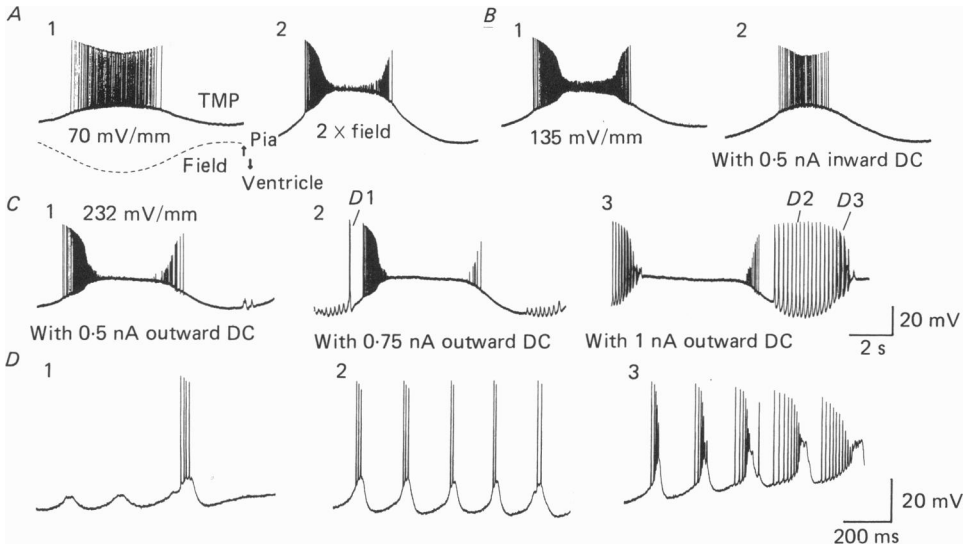

Fig. 5. Interaction between field effect and local current injection in proximal dendritic sites. The responses to large and small external fields (*A* 1 and 2) are compared with the effects of combining field application with local sustained current injections in the inward (*B* 2) and outward (*C*) transmembrane directions. Note the broadening of the somatic plateau and rise in dendritic spike amplitude in *C* 2 and *D* 1 and the superimposition of somatic spikes on dendritic spikes in *C* 3 (details in *D* 2 and 3). Time and voltage scales in *C* apply to *A* and *B*.

All these effects of the injected currents on the active responses to the field are consistent with an additional level of depolarization or hyperpolarization produced by the injected current.

Distal location. At the upper molecular layer (0–180 μm), the passive and active membrane responses to applied fields also appeared to interact additively with responses to injected DC currents (five cells), as illustrated in Fig. 6. Figure 6*A* 1–3 shows the TMP responses to increasing field strength in the absence of injected currents. This recording (at 155 μm) shows responses to fields typical of those described above for this depth, i.e. the baseline TMP polarization and active responses, including small somatic spikes, and a curved (presumably due to weak current shunting by local conductance) somatic plateau in the hyperpolarized phase, dendritic spikes and voltage plateau in the depolarized phase. As we increased the field amplitude, low-amplitude spikes appeared on the dendritic plateau (in the depolarizing phase). A further increase elicited a large-amplitude dendritic spike

superimposed on the later part of the dendritic plateau (Fig. 6*A* 3). In response to increasing field amplitude, the somatic plateau extended in duration.

Figure 6*B* shows a series of membrane responses in the same PC to an applied field of the same amplitude as in Fig. 6*A* 2. While the amplitude of the sinusoidal field was kept constant, an inward DC current (*B* 1), no current (*B* 2) or an outward current (*B* 3) was injected through the cell membrane via the recording microelectrode. With the inward current, the duration of the somatic plateau was diminished, suggesting

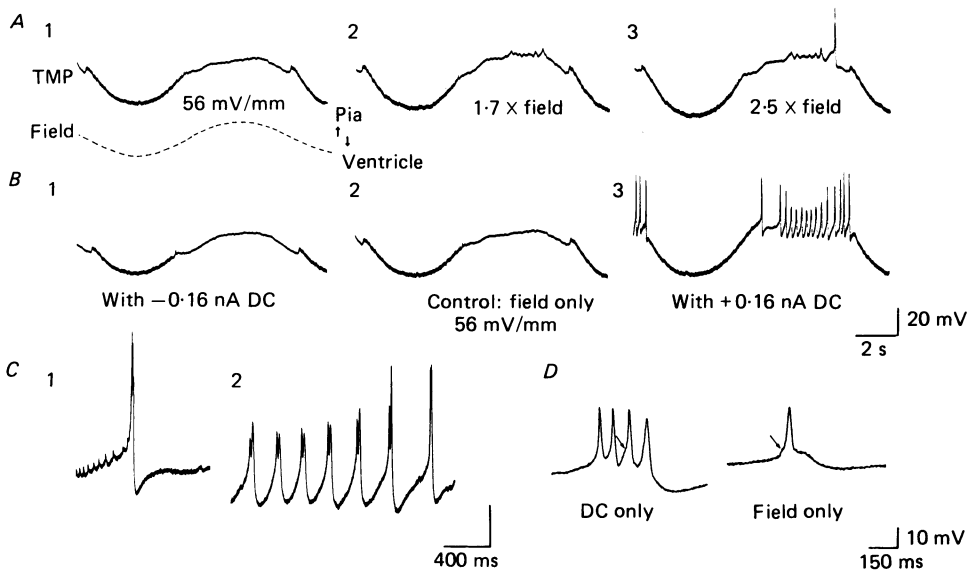

Fig. 6. *A* and *B*, effects of increasing the amplitude of external field (*A* 1–3) are compared to the combined effect of field application and local current injection of inward (*B* 1) and outward (*B* 3) transmembrane directions. Control with field application only is shown in *B* 2. *C*, detail of dendritic spikes in *B* 3, showing small somatic spikes riding on the rising phase of the first dendritic spike (*C* 1) and components of the dendritic spikes that may fail abruptly, resulting in apparently discrete spike amplitudes (*C* 2). *D*, comparison of the threshold voltage level of dendritic spikes elicited by either sustained injection of 1·6 nA outward current or by application of 64 mV/mm external field. Time and voltage scales in *A* same as *B*. Voltage calibration bar in *C* represents same value as in *D*.

that some injected current spread proximally and hyperpolarized the somatic membrane slightly. At the same time, the dendritic plateau shown in *B* 2 (control) is absent in *B* 1 (hyperpolarized), consistent with voltage dependence of the dendritic plateau. In contrast, the effect of outward current shown in *B* 3 is a lengthening of the somatic plateau, and an exaggeration of the dendritic plateau with superimposed dendritic spikes (detail in Fig. 6*C* 1 and 2), similar to those observed during increased external field (cf. Fig. 6*A* 3).

In two PCs tested, the threshold potentials for eliciting dendritic spikes by current injection through a microelectrode at the dendrite or by field application were compared and shown to be identical (e.g. Fig. 6*D*). Since dendritic spikes are generated locally at the distal dendritic region in reptiles (Llinás & Nicholson, 1969; Nicholson & Llinás, 1971; Hounsgaard & Midtgaard, 1988; also this report), as in

mammals (Llinás & Sugimori, 1980*b*), the similarity in voltage threshold seen here suggests that the effect of fields on dendritic spiking is exerted mainly through membrane depolarization; other means of changing the excitability (such as lowering of the spike threshold) are probably not significant.

Mid-dendritic locations. The active responses elicited by external fields at the mid-dendritic locations appear intriguingly complex, even though the passive responses to low-level fields are very small. We will first analyse the responses based on our

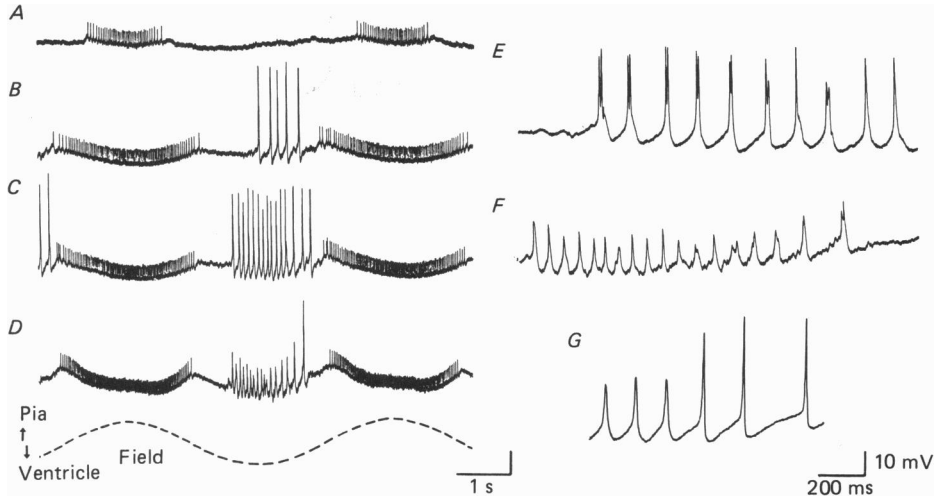

Fig. 7. Mid-dendritic TMP responses to increasing extracellular field strength. *A–D*, responses to progressively greater amplitude of extracellular field. Note that the TMP showed two phases of hyperpolarization in response to each cycle of sinusoidal field. Dendritic spikes were activated despite the hyperpolarized baseline. At higher field strength, failure of some components occurred (*D*). *E–G*, examples of failure of spike components recorded from other PCs. Voltage bar in *D* represents same value as in *G*. Voltage and time scales in *D* apply to *A–C*. Those in *G* apply to *E* and *F*.

findings reported above. We will then report further experiments to confirm these analyses using a combination of field application and current injection, and will show that the complex active responses are consistent with the general scheme of membrane polarization of the PC interacting with voltage-sensitive responses described above.

As in other dendritic regions, the active responses to external fields consisted of Na^+ spikes, Na^+ voltage plateaux, and Ca^{2+} spikes. Their respective phase relationships to the field were also as described above. However, the baseline TMP appeared as dual-phase hyperpolarizing waves dependent on the strength but not on the polarity of the external field. This unexpected pattern is illustrated in a series of responses to increasing fields in Fig. 7*A–D*. Increasing the vertically directed field increased the rate of Na^+ spiking, and the duration and downward curvature of the Na^+ plateau. This is probably due to the depolarization of the PC soma, activating Na^+ spikes and plateau current that spread electrotonically towards the distal pole. The unexpected curvature of the plateau can be interpreted as the summated potential of a distal dendritic hyperpolarization (see Fig. 1*C*) and a proximally

located potential clamp, i.e. the strong Na^+ plateau at the soma. This effectively shifted the neutral point (where depolarization and hyperpolarization cancel out) towards the soma, past the mid-dendritic recording site.

When the field was oriented from the ventricle to the pial surface, Ca^{2+} spikes occurred. They were characterized by multiple components (detail in Fig. 7*E* and *F*), failure of some components at higher field strength (*D–G*) and a higher threshold than Na^+ spikes. Higher fields increased the rate of spiking as well as the amplitude

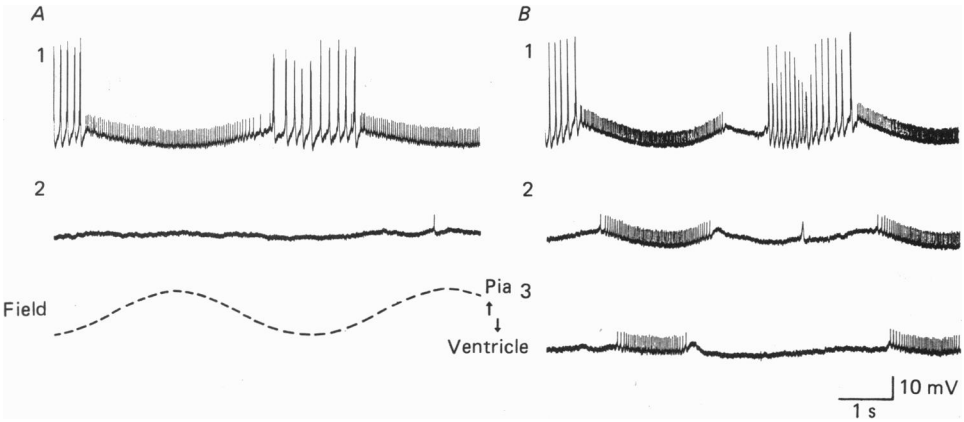

Fig. 8. Interaction between mid-dendritic TMP responses to field and injected DC currents. *A*, responses to a small extracellular field (*A* 1) were blocked by injection of 0·4 nA inward transmembrane current (*A* 2). *B*, TMP responses to a 2× greater field strength (*B* 1) were progressively reduced by 0·4 and 0·8 nA inward DC current (*B* 2 and 3). Same time and voltage scales in *A* and *B*.

of a hyperpolarizing baseline potential. The amplitude was consistently larger than the Na^+ plateau. Again, this can be interpreted as resulting from a summation of a hyperpolarization of the proximal pole and a current shunt at the distal dendrites, in the form of a weak Ca^{2+} plateau.

Another interesting observation was that the discharge of Ca^{2+} spikes actually slowed down at the later stage of the train. This may be a result of the cumulative effect of Ca^{2+}-activated K^+ currents throughout the train.

We were able to test and support our interpretation of the dual-phase hyperpolarizing response at mid-dendritic recording sites by using transmembrane inward currents injected via a micropipette in one experiment. Calcium spikes, and then Na^+ spikes and plateau were suppressed apparently by hyperpolarizing the membrane below the respective thresholds, unmasking a much smaller and simpler baseline perturbation (Fig. 8*A* 2 and *B* 3). The fact that we were able to change the unexpectedly large and dual-phase baseline response by simply suppressing the active responses indicated that the former was not a passive membrane response. Without the shunting effect of plateau conductances at either end of the dendritic axis, this region should be close to the 'neutral point' discussed above, and a small passive response to the field would be expected. This supports the interpretation that the dual-phase hyperpolarization was due to an integration of electrotonically spread active responses from both ends of the dendritic tree.

DISCUSSION

The data from this study show the following findings. (1) External electric fields aligned with the dendritic axis of PCs polarize the cell membrane in ways predicted by a previously proposed theoretical model based on dendritic geometry and cable properties. (2) The polarization of the passive cable structures by fields in turn induces excitation or suppression of active membrane responses signified by spikes and voltage plateaux. The firing patterns of spikes caused by the primary transmembrane response to the fields (i.e. polarization) correspond to modulation patterns of extracellular unit activity by fields we have reported earlier (Chan & Nicholson, 1986). (3) We have utilized field application as an effective tool to characterize the active membrane properties of the turtle PC and to corroborate data from a parallel study using conventional intracellular techniques (Hounsgaard & Midtgaard, 1988).

Primary transmembrane response to external field: polarization of neuronal cable structure

The polarization of neuronal membranes by externally applied DC electric fields has been previously inferred from frequency of spikes and EPSP amplitude (Brookhart & Blachly, 1952; Purpura & McMurtry, 1965; Purpura & Malliani, 1966; Jefferys, 1981; Chan & Nicholson, 1986). In the present study, the transmembrane potential was directly monitored by continuously subtracting from the intracellular potential the large external voltage gradient, i.e. the field, induced in the tissue volume conductor. The latter was recorded by an extracellular microelectrode positioned at approximately the same depth and then carefully adjusted until both micropipettes registered identical extracellular potential during field application before penetration. This was usually quite readily done as field mapping has shown no induced potential gradient in the horizontal plane in the cerebellar tissue when external currents were applied in the pia–ventricle axis (Chan & Nicholson, 1986).

Our experiments show that electric fields applied along the dendritic axis depolarize the half of the dendritic tree toward which the currents are directed, while they hyperpolarize the other half by the same magnitude. Thus, a ventricle-directed field depolarizes the soma and lower dendritic tree while it hyperpolarizes the apical dendrites, whereas a pia-directed field of the same strength polarizes by the same magnitude but in the opposite sense.

While it was not possible to measure the depth profile of polarization in one neurone, a composite profile was drawn from pooled results from a number of neurones penetrated at different depths, with their primary TMP responses normalized to correspond to the same field strength. The normalization is validated by our finding that membrane polarization at a given recording site is proportional to the field strength. The composite profile shows that polarization increases from the middle of the dendrite towards both ends of the dendritic tree. This depth profile is closely approximated by a theoretical curve based on the cable model presented previously (see p. 110, Chan & Nicholson, 1986).

Thus our TMP measurements strongly support the model of a cable structure–field interaction mechanism (Sten-Knudsen, 1960; Ranck, 1975; Chan & Nicholson, 1986;

Tranchina & Nicholson, 1986). On an intuitive level, the model can be visualized as predicting the TMP to arise (in addition to the resting potential) from the difference between two voltage gradients set up by the passage of a current through nervous tissue, which causes ohmic potential drops in two conductive compartments. In one compartment, the extracellular space, the gradient is greater because most of the current passes through this compartment rather than enters the cells. For the same reason, the gradient is smaller in the intracellular space compartment. As a result, the resting potential is reduced (depolarized) by an amount equal to the difference between the two gradients at each location in the half of the cell towards which the current is flowing and conversely increased (hyperpolarized) at each location in the other half. This idea has been explained in fuller detail elsewhere (Ranck, 1975). This model, which is substantiated by the present experimental data, explains the requirement for the fields to be aligned with the major cell axis for optimal modulation of activities to occur in the PC and stellate cells (Chan & Nicholson, 1986), hippocampal neurones (Jefferys, 1981; Richardson, Turner & Miller, 1984) and other central neurones (Rudin & Eisenman, 1954) as well as peripheral fibres (Rushton, 1927). Using actual measurements of TMP responses, the present study is the first confirmation of the mechanism of applied electric field modulation of central neuronal activity, which has so far only been inferred from spiking rate or EPSP amplitudes.

The present experimental data also have interesting implications for some aspects of the cable properties of PCs which are otherwise difficult to assess. Firstly, a key parameter in the equation that describes the polarization depth profile of a uniform cable is its space constant. As shown in Fig. 1*C*, the measured depth profile agrees with the theoretical curve based on a space constant of 260 μm, but not with the other curves shown. Thus an estimate of space constant may be obtained for cells with membrane properties resembling those of a uniform cable. Though only a rough estimation, this approach may be valuable where cells exhibit an unknown amount of electrotonic coupling, so that the geometric considerations become marginally informative.

Secondly, based on a very substantial pool of existing data, it has been recently suggested that the membrane resistance of the PC dendrite is much larger than that of the PC soma (Shelton, 1985). Our results show that the neutral point, where TMP is neither depolarized nor hyperpolarized by the field, is located near the middle of the molecular layer rather than near the soma. Thus, our data suggest that the much larger dendritic membrane surface area relative to the somatic membrane surface could compensate for the effect of the membrane resistance difference. An alternative explanation is that in turtle, the two membrane resistances are not as different as in other species.

Morphological considerations

The depth profile determined in the present study as well as the modulation pattern in PCs reported previously (Chan & Nicholson, 1986) both suggest that the cable structure responsive to the field lies only in the molecular layer. As in most other species studied, the molecular layer in the turtle includes the PC dendrites, but not the axons (Larsell, 1932; Hillman, 1969; Llinás & Hillman, 1969; Palay & Chan-

Palay, 1974). Extensive theoretical considerations of cable structures show, however, that the PC axon, which lies in the same axis as the dendritic tree as in most species (Palay & Chan-Palay, 1974), will contribute to the interaction with the fields and therefore should be integrated into the equivalent cylinder, extending the latter into the granular layer (Tranchina & Nicholson, 1986). But, calculations by these authors also show that the axon's contribution is a cosine function of the angle between the axon and the dendritic axis. Consequently, a PC with an axon that lies at right angle to the dendritic axis would be equivalent to a cylinder that is chopped and sealed at the PC layer. In the frog and a few other species, the PC axon does indeed deviate from the dendritic axis and lie at a right angle in the plane of the PC layer (Hillman, 1969; Llinás & Hillman, 1969). This may be related to the lack of a well-developed white matter layer below the cerebellar cortex, a feature shared by the turtle. Preliminary observation with horseradish peroxidase filling and Golgi staining indicate that this is indeed the case in the turtle cerebellum. This may explain why the axon apparently fails to capture any of the applied field.

Active responses to externally applied field

The primary TMP responses, i.e. the changes in baseline voltage levels, are linearly related to field amplitude up to the level at which action potentials appear. Further increases in field strength cause asymmetry of response to the two polarities. The hyperpolarizing response continues to rise linearly with the field strength, but the depolarization does not increase as much. At higher field strength, action potentials discharge at higher rates and voltage plateaux appear in the depolarizing phase. When these active responses are removed by appropriate pharmacological blockers, the linear relationship to field strength in the depolarizing phase is unmasked. These observations suggest a strong interaction between the active and passive responses. The action potentials seem to be triggered by the depolarizing displacement of the baseline TMP response as evidenced by the definite threshold voltage levels.

In the hyperpolarizing phase, spikes and plateaux are also observed, but the spikes are of lower amplitude and slower rise time. The plateaux, if present, are of lower amplitude and conform more to the curvature of the TMP baseline. These features indicate that they are electrotonically spread from other parts of the cell. This observation fits in with the picture that while one half of the cable structure becomes hyperpolarized by the field, the other half becomes depolarized.

The shape of all the plateaux and spikes varies with respect to the location of recording. These and other data from the present study show that in the proximal half of the PC, large, fast, Na^+-dependent action potentials and Na^+-dependent voltage plateaux are elicited by the tonic, passive depolarization induced by external fields. The amplitude of the fast spikes gradually decreases towards the distal portion of the cell, indicating the proximal (somatic and possibly primary dendritic) origin of these spikes. Likewise, the Na^+-dependent voltage plateau is proximally originated and electrotonically spread to the distal dendrites. Ca^{2+}-dependent spikes, which are broader and usually notched, as in the alligator, suggesting saltatory conduction down the dendrite (Nicholson & Llinás, 1971), are generated in the distal half of the dendritic tree. They have a much higher threshold than Na^+-dependent spikes, and seem to be electrotonically spread to the soma from the most proximal dendritic 'hot

spot'. A weak Ca^{2+}-dependent plateau is generated in the distal dendrites and typically does not spread very far proximally. The characteristics of these field-induced active components are similar to those elicited by the current injection technique in the turtle PC (Hounsgaard & Midtgaard, 1988), and also bear resemblances to those described in the mammalian PC (Llinás & Sugimori, 1980*a*, *b*), but for the fact that the Ca^{2+} plateau is less dominant in the turtle. When Na^+ spikes were activated to fire by external field or current injection to beyond 160 spikes/s, the spikes were inactivated, and at the same time, the TMP showed a voltage plateau distinct from the Na^+-dependent plateau described above. This plateau was more depolarized and also Na^+ dependent.

The results obtained by differential polarization of the somatic and distal dendritic regions of turtle PCs provide important support for the proposal that the transient hyperpolarization and Ca^{2+} spikes are active responses confined to the spiny dendrites (Hounsgaard & Midtgaard, 1988).

It appears that the primary TMP response is the direct cause for most of the active responses. Below the TMP level at which voltage plateaux are well developed the firing rate appears to be a function of the TMP baseline. Beyond that level the duration of the plateaux, as well as the firing rate of action potentials, increases with the amplitude of the extracellular field, the TMP baseline having become a constant voltage plateau. These voltage plateaux seem also to be triggered by TMP levels.

Corroboration with extracellular unit modulation pattern

The active TMP responses described in this report help clarify the nature of the modulation pattern of extracellular PC units by external fields (Chan & Nicholson, 1986). In both distal dendritic and proximal levels, most PC units are activated or accelerated by fields directed towards the soma. By their phase relationship to the fields and other features of temporal pattern, these units are correlated to Na^+-dependent, somatically originated spikes that are recordable as giant spikes in proximal as well as distal dendritic levels. Those extracellular spikes that are activated by both field directions probably represent two different types of action potentials. Na^+ spikes are activated by ventricle-directed fields while Ca^{2+} spikes are activated by pial surface-directed fields. The acceleration of Na^+ spikes riding on the slower-rising slope of the Ca^{2+} spike, as well as the silence after the discharge (presumably due to a Ca^{2+}-activated K^+ conductance) of the Ca^{2+} spike, which is illustrated in Fig. 5*D* in this report, find a parallel extracellular discharge pattern in a PC responding to fields directed towards the pial surface (see Fig. 5*F* and *H* in Chan & Nicholson, 1986). The previous finding that most PC units are activated by ventricle-directed fields but not pia-directed fields is consistent with the much higher threshold for Ca^{2+} spikes found in this study. The amplitudes of fields used in that previous study were generally lower.

The plateau associated with Na^+ spike inactivation reported here may be correlated to a period of non-spiking or spikes of much lower amplitude in extracellular recording elicited by a high-amplitude field directed towards the ventricle. This period is also preceded and followed by taller spikes discharging at about 160 spikes/s (C.Y. Chan & C. Nicholson, unpublished data).

Interaction of field-induced and current injection-induced effects

We have presented data from a series of experiments showing that the polarization caused by applied fields is independent and additive to the polarizing effects of current injection through the intracellular microelectrode. This provides further evidence that the action of applied fields on the excitability of neurones is simply expressed as polarization of neuronal membrane. Furthermore, since the two modes of polarization are different in nature, they prove to be mutually complementary as cell electrophysiological tools. For instance, different regions of cell membrane can be polarized by the two methods. The field application approach is especially interesting in that regions remote from the intracellular electrode can be polarized at will, and the other end of the cell will be polarized in the opposite sense, thus confining the voltage manipulation spatially, even within one cell. All these can be undertaken by the experimenter without being dependent on electrode placement at particular regions of a cell, which may be difficult.

Our experiments showed that interesting information can be obtained from the interaction of these two modes of polarization. For instance, we were able to determine the nature of the curious dual-phase hyperpolarization observed in the mid-dendritic region of PC in response to field application. This was achieved by injecting an inward current step to suppress all the active responses, showing a very low-amplitude sinusoidal tonic TMP baseline response, and indicating that the extra hyperpolarizing curvature had been due to a strong, remote current shunt at one end of the cell that had effectively moved the neutral point by changing local cable properties.

Our data from a recent study utilizing this combined approach to investigate synaptic electrophysiology in the turtle PC will be reported in a separate publication.

This work was supported by the U.S. National Institute of Health Grants NS 18287 and NS 13742 from NINCDS. C. Cronin provided technical assistance and S. Sleet assistance in photography.

REFERENCES

BROOKHART, J. M. & BLACHLY, P. H. (1952). Cerebellar unit responses to D.C. polarization. *American Journal of Physiology* **171**, 711.

CHAN, C. Y., HOUNSGAARD, J. & NICHOLSON, C. (1985). Induced responses of transmembrane potential to externally applied electric fields in turtle Purkinje cells. *Society for Neuroscience Abstracts* **11**, 689.

CHAN, C. Y. & NICHOLSON, C. (1986). Modulation by applied electric fields of Purkinje and stellate cell activity in the isolated turtle cerebellum. *Journal of Physiology* **371**, 89–114.

GAUTHIER, C., MOLLICA, A. & MORUZZI, G. (1956). Physiological evidence of localized cerebellar projections to bulbar reticular formation. *Journal of Neurophysiology* **19**, 468–483.

HEISEY, S. R. (1970). Cerebrospinal and extracellular fluid spaces in turtle brain. *American Journal of Physiology* **219**, 1564–1567.

HILLMAN, D. E. (1969). Neuronal organization of the cerebellar cortex in amphibia and reptilia. In *Neurobiology of Cerebellar Evolution and Development*, ed. LLINÁS, R., pp. 279–325. Chicago: American Medical Association, Education and Research Foundation.

HOUNSGAARD, J. & MIDTGAARD, J. (1988). Intrinsic determinants of firing pattern in Purkinje cells of the turtle cerebellum *in vitro*. *Journal of Physiology* **402**, 731–749.

JEFFERYS, J. G. R. (1981). Influence of electric fields on the excitability of granule cells in guinea-pig hippocampal slices. *Journal of Physiology* **319**, 143–152.

LARSELL, O. (1932). The cerebellum of reptiles: Chelonians and alligator. *Journal of Comparative Neurology* **56**, 299–345.

LLINÁS, R. & HILLMAN, D. E. (1969). Physiological and morphological organization of the cerebellar circuits in various vertebrates. In *Neurobiology of Cerebellar Evolution and Development*, ed. LLINÁS, R., pp. 431–465. Chicago: American Medical Association, Education and Research Foundation.

LLINÁS, R. & NICHOLSON, C. (1969). Electrophysiological analysis of alligator cerebellar cortex: A study of dendritic spikes. In *Neurobiology of Cerebellar Evolution and Development*, ed. LLINÁS, R., pp. 431–465. Chicago: American Medical Association, Education and Research Foundation.

LLINÁS, R. & SUGIMORI, M. (1980*a*). Electrophysiological properties of *in vitro* Purkinje cell somata in mammalian cerebellar slices. *Journal of Physiology* **305**, 171–195.

LLINÁS, R. & SUGIMORI, M. (1980*b*). Electrophysiological properties of *in vitro* Purkinje cell dendrites in mammalian cerebellar slices. *Journal of Physiology* **305**, 197–213.

NICHOLSON, C. & LLINÁS, R. (1971). Electrophysiological properties of dendrites and somata in alligator Purkinje cells. *Journal of Neurophysiology* **34**, 532–551.

PALAY, S. L. & CHAN-PALAY, V. (1974). In *Cerebellar Cortex, Cytology and Organization*, pp. 216–233. New York: Springer-Verlag.

PURPURA, D. P. & MCMURTRY, J. G. (1965). Intracellular activities and evoked potential changes during polarization of motor cortex. *Journal of Neurophysiology* **28**, 166–185.

PURPURA, D. P. & MALLIANI, A. (1966). Spike generation and propagation initiated in dendrites by trans-hippocampal polarization. *Brain Research* **1**, 403–406.

RANCK JR, J. B. (1975). Which elements are excited in electrical stimulation of mammalian central nervous system? A review. *Brain Research* **98**, 417–440.

RICHARDSON, T. L., TURNER, R. W. & MILLER, J. J. (1984). Extracellular fields influence transmembrane potential and synchronization of hippocampal neuronal activity. *Brain Research* **294**, 255–262.

RUDIN, D. O. & EISENMAN, G. (1954). The action potential of spinal axons *in vitro*. *Journal of General Physiology* **37**, 505–538.

RUSHTON, W. A. H. (1927). The effect upon the threshold for nervous excitation of the length of nerve exposed and the angle between current and nerve. *Journal of Physiology* **63**, 357–377.

SHELTON, D. P. (1985) Membrane resistivity estimated for the Purkinje neuron by means of a passive computer model. *Neuroscience* **14**, 111–131.

STEN-KNUDSEN, O. (1960). Is muscle contraction initiated by internal current flow? *Journal of Physiology* **151**, 363–384.

TRANCHINA, D. & NICHOLSON, C. (1986). A model for the polarization of neurons by extrinsically applied electric fields. *Biophysical Journal* **50**, 1139–1156.